

Assistance to bone milling: a tool mounted visual display improves the efficiency of robotic guidance

Vincent Françoise, Anis Sahbani, Agnès Roby-Brami, Guillaume Morel

Abstract—In this paper, a new kind of assistance for bone milling is disclosed. It combines a robotic comanipulator applying forces to guide the milling tool tip with a visual display mounted on the hand-held tool. This visual display is a LED bargraph providing to the user a geometric information that is mostly redundant with the forces exerted by the robot, thus constituting a multi-modal feedback. Although very basic and rather inexpensive, the additional visual display is experimentally shown to significantly improve the precision of the gesture.

I. INTRODUCTION

Robotic assistance to bone milling is a major issue in the development of computer-assisted orthopedic surgery. Among the propositions found in the literature in this domain, the comanipulation approach, in which both the robot and the surgeon manipulate the same tool, is of particular interest, [1], [2], [3], [4]. With this approach, a preoperative planning is performed in order to determine the bone region to be removed by milling. This defines a virtual limit between the region to be removed and the region to be preserved. Typically, this limit fits the shape of a prosthesis to be implanted. During the operation, after proper registration, the robot prevents the surgeon for milling bone regions that must be preserved by applying resistive forces when the virtual limit is violated. Two comanipulators designed for assistance to bone milling are today available for clinical practice: Makoplasty [5] and Acrobot [6].

Advantages of comanipulation are numerous: the surgical flow and the surgical gesture are both largely preserved as compared to conventional interventions; the tool control is left to the surgeon for dealing with unpredicted situations; the precision of the gesture is proven to be improved in the literature as compared to no assistance [6]; the approach can be easily coupled with existing navigation systems for registering and tracking the milling tool with respect to the bone [5].

In previous publications (see *e.g.* [7]), we have disclosed a comanipulator for assistance to bone milling, called *Surgicobot*. The question of the precision has been emphasized by measuring how much naive subjects overpass a virtual limit during assisted milling tasks. It was observed that during comanipulated bone milling, the forces exerted by the robot are summed with the forces exerted by the bone on the tool (typically from 5 to 10 N), which makes it difficult for the user to finely feel the robot indications.

In order to increase the force guidance efficiency, a new approach is proposed in this paper. It consists in mounting a visual display – namely a LED bargraph – near the milling tool

UPMC Univ Paris 06, CNRS UMR 7222, ISIR,F-75005, Paris, France
francoise, sahbani, roby-brami, morel@isir.upmc.fr

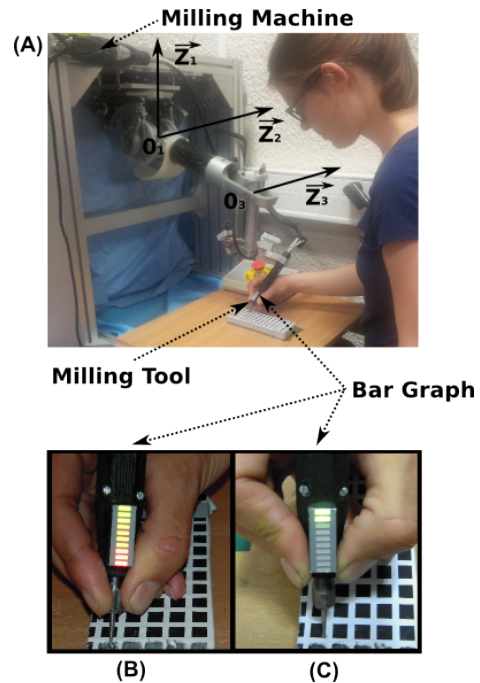


Figure 1. (A) Surgicobot; (B-C) Zoom on the milling tool equipped with a LED bargraph displaying two different indications.

tip. The LED bargraph simply displays the distance between the tool tip and the virtual limit, see Fig. 1. The results provided in this paper aims at proving, when considering a canonical milling task of a planar surface, that this approach allows for increasing the overall gesture precision.

This paper is organized as follows. Section II describes Surgicobot, the LED bargraph display implementation and the testbed. Methods used to generate active constraints, to program the LED bargraph, and to evaluate the performances are detailed in Sec. III. Experimental results are given in Sec. IV and discussed in Sec. V. Finally, conclusion and perspectives are given in Sec. VI.

II. EXPERIMENTAL SETUP

A. Surgicobot

Surgicobot is a comanipulator designed to assist an orthopedic surgeon during a milling task. It is mounted on a bridge support placed above the table and holds the milling tool in such a way that it can also be grasped by the surgeon, see Fig. 1-A. The Surgicobot kinematic structure is composed of a 3 Degrees of Freedom (DOF) passive wrist mounted on a 3DOF active arm. The active arm comprises DC motors, low

friction transmissions and springs that balance the weight of both the tool and the wrist, in such a way that Surgicobot offers very high backdrivability. As a result, when the current in the DC motors is null, the milling tool is free of moving along any DOF.

As detailed in [7], the three passive pivot joints constituting the passive wrist permanently intersect at the tip of the milling tool mounted on the wrist last body, in such a way that Surgicobot is able to generate controlled pure forces (no torque) at the tool tip. Due to low friction and inertia, the force exerted at the tool tip can be controlled in open loop by proper computation of the joint torque :

$$\tau_a = \mathbf{J}_v^T \mathbf{f} , \quad (1)$$

where $\tau_a \in \mathbb{R}^3$ is the torque vector applied to the three active joints, \mathbf{f} is the force to be applied at the tool tip and $\mathbf{J}_v \in \mathbb{R}^{3 \times 3}$ is the reduced Jacobian matrix of the robot.

B. LED bargraph

A LED bargraph is fixed on the milling tool in order to display an information as illustrated in the Fig.1B and 1C. The display is positioned in such a way that it does not affect the grasping of the milling tool, while it fits within the surgeon's field of view. The LED bargraph is composed of 10 LEDs with three different colors: 3 LEDs are green, 4 are orange and 3 are red. The algorithm that is used to lighten the LEDs depending on the position of the tool tip with respect to the virtual limit is detailed in Sec. III.

C. Task

In this paper, in order to evaluate the efficiency of several modes of assistance, a canonical milling task is considered. In this testbed, the tool tip is a 1.1 mm radius spherical drill whose center coincides with Surgicobot's wrist center.

The test task consists of milling $7 \times 7 \times 2$ mm parallelepipeds out of a thick block made with GPVC (Grey PolyVinyl Chloride) material and exhibiting a planar horizontal upper surface, see Fig. 2. The combination of the milling tool, its rotation speed, and the GPVC material has been chosen in such a way that the forces involved to mill, as well as the velocity of the milling process, are similar to those encountered during bone milling with surgical tools.

The horizontal limit of the region to be removed is delimited by a black square drawn on the GPVC block surface, while only the limit in depth is displayed to the subject by either applying a vertical resistive force, or lightening the LED bargraph LEDs, or both.

III. METHODS

A. Force feedback

Surgicobot is programmed to impose an impedance-type virtual wall. To do so, the tool tip point T is projected into the closest point M belonging to the limit surface, see Fig. 2B.

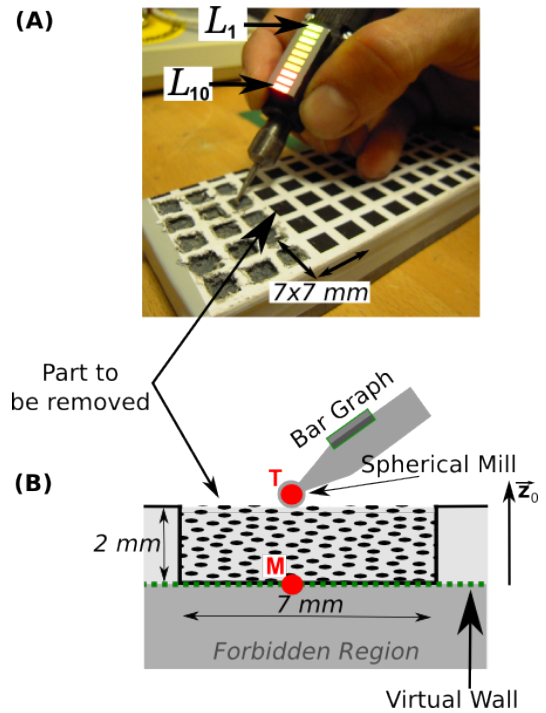


Figure 2. Experimental set up; (A) A top view of the testbed; (B) A lateral schematic cross section of the testbed.

Denoting \mathbf{n} the normal vector to the limit surface at point M , oriented toward the free region, one sets:

$$\overrightarrow{TM} = -p\mathbf{n} , \quad (2)$$

where p is the signed distance from T to the limit surface. Note that $p > 0$ when T is in the free region. A repulsive force \mathbf{f} is then computed by:

$$\mathbf{f} = \begin{cases} (Kp + B\dot{p})\mathbf{n} , & \text{if } p < 0 \\ 0 , & \text{otherwise} \end{cases} , \quad (3)$$

where \dot{p} is computed by numerically differentiating p , K is the stiffness and B is the viscosity. Increasing K allows to produce higher guiding forces, but it may lead to instability, which is difficult to predict as it also depends on the user's impedance. In order to tune the control gains, a set of basic experiments were performed with several subjects. It was experimentally found that setting $K = 10kN.m^{-1}$ and $B = 50N.s.m^{-1}$ provided unconditional stability with enough margin.

B. Visual feedback

In this section, the algorithm for turning on and off the LEDs of the LED bargraph depending on the signed distance p is explained.

The LEDs are numbered from the upper green LED L_1 to the lower red LED L_{10} , see Fig. 2. When $p = 0$, *i.e.* when the tool tip coincides with the limit, all the green and orange LEDs (L_1 to L_7) are turned on, while the red LEDs (L_8 to L_{10}) are turned off. If p becomes negative, L_8 to L_{10} are progressively turned on to indicate that the limit is overpassed. On the

contrary, when p becomes positive, L_7 to L_1 are progressively turned off, indicating that the limit is not reached yet. In other words, the algorithm for determining the state of L_i is:

$$\text{state}(L_i) = \begin{cases} \text{ON, if } p < (8-i)\delta \\ \text{OFF, otherwise} \end{cases}, \quad (4)$$

where δ is a positive scalar distance tuning the sensitivity of the device. Again, tuning δ was performed thanks to a set of preliminary experiments with naive subjects. A value $\delta = 0.2$ mm was found to be optimal: larger values led to decrease the precision while for smaller values, some subjects found the device too sensitive and oscillations were observed due to excessive reaction by the user.

C. Experimental protocol

Experiments have been conducted with 10 naive subjects, men and women, aged 22-30. Each subject accomplishes the test task under three different conditions. Condition (1) involves force feedback only, Condition (2) involves both force feedback and visual feedback, Condition (3) involves visual feedback only. Note that the sequencing of the three conditions is randomly established for each subject in order to avoid possible bias due to a learning effect.

The duration of each trial is limited to 40 seconds, after which the milling tool is automatically turned off. This duration was found sufficient to achieve the task, whereas unlimited time credit could lead subjects who feel uncomfortable with a given mode of assistance to exaggeratedly slow down, thus biasing the precision evaluation.

D. Performance assessment

To quantify the performance of a given subject, the tool tip position \mathbf{x} is first recorded every millisecond. For a given trial, n values of \mathbf{x} are thus recorded, noted \mathbf{x}_k , $k \in \{1, \dots, n\}$. Figure 3 is an example record of the tool penetration $p = \mathbf{x}^T \mathbf{z}_0$ (\mathbf{z}_0 being the vertical vector pointing upwards), for one same subject performing the task under two different conditions. On this example, it is visually clear that the subject, under Condition (2), better respects the virtual limit than he does under Condition (1). In order to provide a mean for quantitatively comparing the performance between two trials, five indexes are used.

It is first interesting to evaluate how frequently and how far the limit is overpassed. This is made by computing for each time sample the distance p_i and by selecting among the n values of p_i those that are negative. A subset of $m < n$ negative values of p_i is built, from which three indexes are computed: the maximal penetration in the forbidden region p_{\max} , the mean penetration in the forbidden region \bar{p} , and the total time spent in the forbidden region during the task, t_{tot} :

$$p_{\max} = \max_{j=1..m} (|p_j|), \quad \bar{p} = \frac{1}{m} \sum_{j=1}^m |p_j|, \quad \text{and} \quad t_{\text{tot}} = m.T, \quad (5)$$

$T = 10^{-3}$ s being the sampling time. Note that all these three indicators should be minimized for performance optimization.

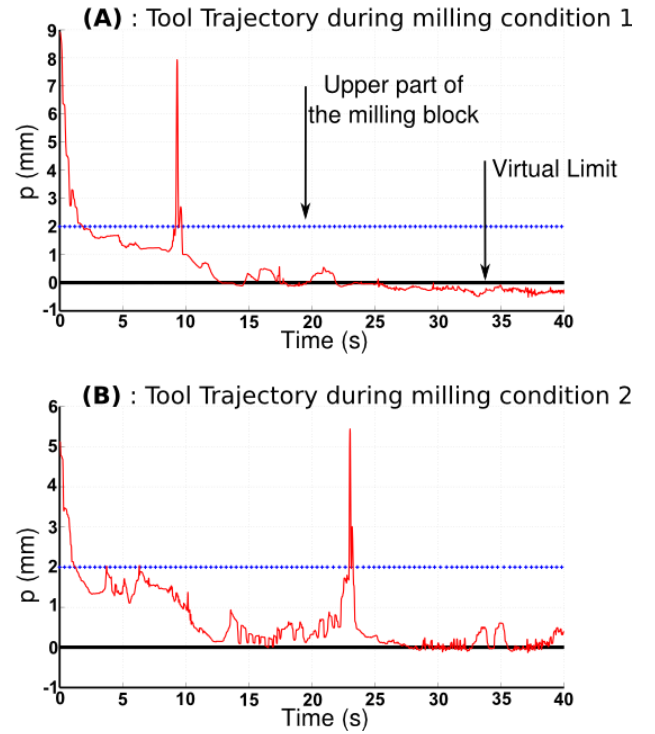


Figure 3. An example of the tool trajectories during two different milling task conditions. (A) Condition (1); (B) Condition (2)

Moreover, the total volume covered by the milling tool during an experimental trial is the union of the individual spherical volumes S_i occupied by the tool at position \mathbf{x}_i :

$$S = \bigcup_i S_i(\mathbf{x}_i) \quad (6)$$

Note that spherical volumes could be estimated after each task using the recorded positions of the tool tip and a voxelization of the environment.

From S , one computes two extra performance indexes, which are the total volume v_{tot} of GPVC material removed in the authorized region and the volume v_f of GPVC material removed in the forbidden region. They are computed by:

$$v_{\text{tot}} = \text{measure}(S \cap S_b) \quad \text{and} \quad v_f = \text{measure}(S \cap S_f), \quad (7)$$

where S_b and S_f are the 3D volumes occupied by the region to be removed and by the forbidden region, respectively. A perfect realization of the task is when $v_{\text{tot}} = 98 \text{ mm}^3$ while $v_f = 0$.

All the five indicators (p_{\max} , \bar{p} , t_{tot} , v_{tot} and v_f) are averaged across subjects for each of the three conditions defined in the protocol. These indicators are analyzed with one factor (condition) analysis of variance (ANOVA)¹.

¹ANOVA is a test for checking if a given conclusion made by comparing the mean values of an experimental measure (here, any of the 5 indexes) computed for different categories (here the 3 conditions), is statistically significant. It provides two main numbers: the F -value whose large values indicate large differences between the categories, and a p -value, which measures the statistical significance. The p -value should be typically smaller than 0.01 to conclude that there is a statistically significant difference between the means of the categories. See e.g. [8].

IV. RESULTS

Figure 4 displays the total volume removed in the free region, averaged across the ten subjects, for the three different conditions.

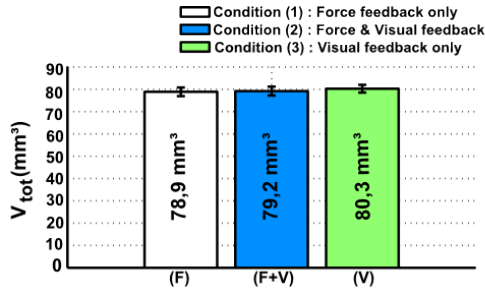


Figure 4. Volume v_{tot} removed in the free region, averaged across the 10 subjects.

We observe almost the same average values for v_{tot} under the three conditions. The hypothesis that the condition does not affect the mean volume v_{tot} is confirmed with a one factor ANOVA test, which provides $F = 0.26$, $p = 0.7752$. In other words, the condition (force feedback, visual feedback, or both) does not significantly affect the efficiency of milling, nor does it slow down the gesture.

Figure 5 presents the evaluation of the four indexes quantifying the intrusions in the forbidden region : \bar{p} , p_{max} , t_{tot} and v_f . A visual inspection shows that Condition (2) clearly outperforms the two other conditions for all the four indexes.

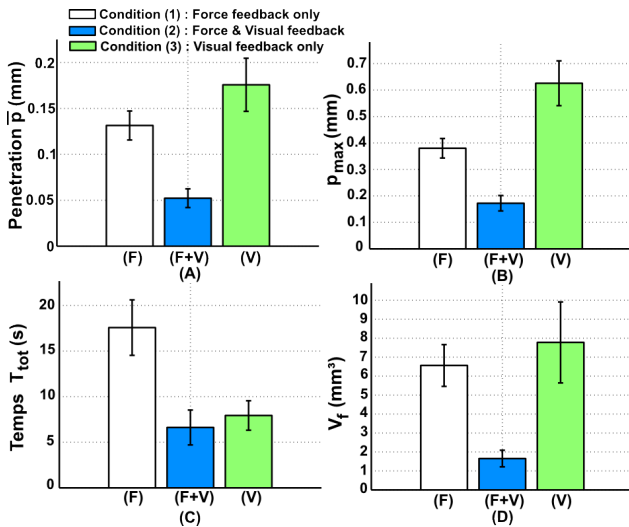


Figure 5. Comparison of the indexes quantifying the penetration in the forbidden region under the 3 conditions: (A) mean penetration \bar{p} ; (B) maximal penetration p_{max} ; (C) total time t_{tot} ; (D) removed forbidden volume v_f . Indexes are averaged across the 10 subjects.

More precisely, comparing Condition (2) to Condition (1), it is observed that adding visual feedback to force feedback leads to reduce by 60% the index \bar{p} , by 55% the index p_{max} , by 77% the index t_{tot} and by 75% the index v_f . Comparing Condition (2) with Condition (3), it is observed that adding

force feedback to visual feedback leads to reduce by 70% the index \bar{p} , by 72% the index p_{max} , by 40% the index t_{tot} and by 79% the index v_f .

All these observations are statically significant since a one factor ANOVA, with subjects as repeated measures, showed a significant effect: ($F = 14.9$, $p = 0.0002$), ($F = 21.7$, $p < 0.0001$), ($F = 15.4$, $p = 0.0001$) and ($F = 8.36$, $p = 0.0027$), respectively for \bar{p} , p_{max} , t_{tot} and v_f .

V. DISCUSSION

In the previous section, an experimental analysis of robotic guidance during a milling task has been detailed. Presented results demonstrate that when force and visual feedback are simultaneously associated, the accuracy of the milling is significantly increased (reduction of the intrusions in the forbidden region) without altering the quality of the achieved task (preservation of the amount of removed material).

Imposing a time limit for the task completion, as well as instructing the subjects to remove as much material as possible without violating the constraint during this limited time, are probably determinant factors in the results presented in Fig. 4, which emphasize an equal volume of removed material for the three conditions. This choice was deliberate in order to be able of further comparing the other indexes of performance that quantify the intrusions in the forbidden region. At a price, it shall be clear that these instructions placed the subjects under conditions that do not strictly reproduce those of a surgical operation. Moreover, GPVC material that has been tested in this experimentation does not encompass all the range of bone tissue stiffnesses, which should be kept in mind for discussing the results. Nevertheless, the experiments exhibit clear results with strong statistical significance, which allow to compare the modes of assistance with a good confidence that they will apply to a real situation during bone surgery.

In fact, this study illustrates the contribution of multimodal sensory information for the regulation of action. It is well known that visual information contributes in reducing the uncertainty of the motor output in relation to the task [9]. For example, in an isometric force production task, the addition of visual feedback decreases the fluctuations in isometric force production suggesting that it cannot be guided accurately by proprioceptive and tactile feedback alone. Both spatial (definition and gain) and temporal (intermittency) properties of visual information can modify the accuracy of movement control [10]. There are optimal ranges of visual parameters in both spatial and temporal domains of visual information that combines to decrease the variability of force output [11]. In our study, we used a visual feedback with a large gain (2.5 cm LED bargraph represents 2mm depth) but a coarse spatial (10 steps) definition. However, in contrast to the situation of isometric force production tasks quoted above, the modulation of the visual feedback was here included in a voluntary action (milling).

The addition of visual and force feedback induces a significant improvement of milling accuracy by reference to isolated force or visual feedback alone. This effect is probably due to

a combination of perceptive cues to guide the milling action [12]. This combination of force feedback and visual information reduces error incidence and excessive force application in a variety of situations, making interaction feel more natural and easing the cognitive burden on the operator [13]. Note that with the proposed device, the visual information is spatially close to the working point of the action. This probably participates to enhancing the perception of the progression of the milling task, by reference to the natural proprioceptive and visual monitoring of the action. Both the spatial congruence of the feedback and its temporal coupling within the perception-action cycle probably contribute to its beneficial effect [14]. To confirm the last assumption, a comparison of the LED bargraph with a conventional (GUI) visualization system (navigation system) should be investigated, which is left to future works. Also, the use of directional information instead of a one dimensional LED bargraph displaying the force intensity could be evaluated. The question here is to verify if a complete force indication (magnitude and direction) is beneficially completed by a one dimensional visual information (intensity only), which would allow to keep the visual display device simple and inexpensive.

It is noteworthy that the perception are not simultaneous but sequential since the visual feedback precedes the force feedback. This temporal sequence is reinforced by the color code since the orange light signals a warning. The force feedback appears synchronously with the red visual feedback and they increase in parallel when the milling tool is inside the virtual limit. It is thus likely that the visual feedback acts not only to enhance the perception of the haptic feedback but also as a warning signal. Multimodal warning signals have already demonstrated their effect in other activities, for example for driving, providing both temporal and spatial coherence [15], [16]. The visual signal probably directs the attention of the user in order to both increase and speed the haptic perception [17].

VI. CONCLUSION AND FUTURE WORK

Experimental results presented in this paper clearly demonstrate that associating force and visual feedback significantly improves the accuracy of the milling process. As emphasized in the discussion section, this result is largely consistent with a number of experimental observations on the effect of multimodal feedback published in the neurosciences literature.

Further investigations are to be programmed, to determine the influence of visually displaying the force direction during multi-directional operations, to evaluate the reproducibility of the result for different material stiffnesses, as well as to confirm the importance of the observed effect when expert subjects – namely orthopedic surgeons – perform the experiments instead of naive subjects.

REFERENCES

[1] G. Brandt, A. Zimolong, L. Carrat, P. Merloz, H. W. Staudte, S. Lavallée, K. Radermacher, and G. Rau, "Crigos: a compact robot for image-guided orthopedic surgery," *IEEE Transactions on Information Technology in Biomedicine*, vol. 3, no. 4, pp. 252–260, 1999.

[2] R. Taylor, B. Mittelstadt, H. Paul, W. Hanson, P. Kazanzides, J. Zuhars, B. Williamson, B. Musits, E. Glassman, and W. Bargar, "An image-directed robotic system for precise orthopaedic surgery," *IEEE Transactions on Robotics and Automation*, vol. 10, no. 3, pp. 261–275, 1994.

[3] A. Wolf and B. Jaramaz, "Mbars: Mini bone attached robotic system for joint arthroplasty," in *IEEE/RAS-EMBS International Conference on Biomedical Robotics and Biomechatronics*, Pisa, 2006, pp. 1053–1058.

[4] A. Hein and T. Lueth, "Control algorithms for interactive shaping [surgical robots]," in *Robotics and Automation, 2001. Proceedings 2001 ICRA. IEEE International Conference on*, vol. 2, 2001, pp. 2025 – 2030 vol.2.

[5] A. Pearle, D. Kendoff, V. Stueber, V. Mushal, and J. Repicci, "Perioperative management of unicompartmental knee arthroplasty using the mako robotic arm system (makoplasty)," *The American journal of orthopedics*, vol. 38, no. 2S, pp. 16–19, 2009.

[6] M. Jakopec, F. Rodriguez y Baena, S. J. Harris, P. Gomes, J. Cobb, and B. Davies, "The hands-on orthopaedic robot "acrobot": Early clinical trials of total knee replacement surgery," *IEEE Transactions on Robotics and Automation*, vol. 19, no. 5, pp. 902–911, 2003.

[7] V. Francoise, A. Sahbani, and G. Morel, "A comanipulation device for orthopedic surgery that generates geometrical constraints with real-time registration on moving bones," in *IEEE International Conference on Robotics and Biomimetics (ROBIO'11)*, Phuket Island, Thailand, 2011, pp. 38–43.

[8] H. Scheffé, *The Analysis of Variance*. John Wiley & Sons, 1959.

[9] J. M. Hillis, M. O. Ernst, M. S. Banks, and M. S. Landy, "Combining sensory information: mandatory fusion within, but not between, senses," *Science*, vol. 298, no. 5598, pp. 1627–30.

[10] J. J. Sosnoff and K. M. Newell, "Intermittency of visual information and the frequency of rhythmical force production," *J Mot Behav*, vol. 37, no. 4, pp. 325–34.

[11] S. L. Hong, A. J. Brown, and K. M. Newell, "Compensatory properties of visual information in the control of isometric force," *Percept Psychophys*, vol. 70, no. 2, pp. 306–13.

[12] M. O. Ernst and M. S. Banks, "Humans integrate visual and haptic information in a statistically optimal fashion," *Nature*, vol. 415, no. 6870, pp. 429–33.

[13] M. Massimino and T. Sheridan, "Teleoperator performance with varying force and visual feedback," *Human Factors: The Journal of the Human Factors and Ergonomics Society*, vol. 36, no. 1, pp. 145–157, 1994.

[14] M. O. Ernst and H. Blthoff, "Merging the senses into a robust percept," *Trends Cogn Sci.*, vol. 8, no. 4, pp. 162–169, 2004.

[15] C. Ho, N. Reed, and C. Spence, "Multisensory in-car warning signals for collision avoidance," *Hum Factors*, vol. 49, no. 6, pp. 1107–14.

[16] M. N. Lees, J. Cosman, J. D. Lee, S. P. Vecera, J. D. Dawson, and M. Rizzo, "Cross-modal warnings for orienting attention in older drivers with and without attention impairments," *Appl Ergon*, vol. 43, no. 4, pp. 768–76.

[17] C. Spence and C. Parise, "Prior-entry: a review," *Conscious Cogn*, vol. 19, no. 1, pp. 364–79.